ChemComm

ROYAL SOCIETY OF CHEMISTRY

FEATURE ARTICLE

View Article Online
View Journal

Cite this: DOI: 10.1039/d5cc06562c

Design of metabolism-inspired hydrogels driven by emergence of function

Kosuke Okeyoshi *[a] and Ryo Yoshida [b]

In the 21st century, bioinspired hydrogels have been developed using stimuli-responsive polymer networks in aqueous environments. In this review, "metabolism-inspired hydrogels" are discussed, focusing on the symbolic functions of living organisms. Considering that cell activities in animals and plants are driven by cyclic chemical reactions such as TCA cycle or Calvin–Benson cycle, catalyzed by multiple enzymes, we discuss artificial hetero-systems, especially, self-oscillating gel and artificial photosynthetic gel designs. By providing the necessary materials or photoenergy to gels, they can be converted into useful substances or mechanical energy. These gels can be categorized as chemomechanical or energy-converting gels. Copolymer networks with a redox catalyst convert substances and energy by acting as an active network during the phase transition of the polymer. The polymer itself is not necessary for the chemical reactions, but it acts as a critical active mediator for the emergence of function. To construct polymer networks, functional molecules or catalytic nanoparticles can be integrated using simple methods. This review focuses on the methodology for network design and stepwise integration. In the future, synthetic technologies, such as precise polymerization, are expected to promote a range of self-organized morphologies and efficient energy conversion. We hope that the discussions in this review will help leverage the huge potential of polymer networks in the development of soft materials.

Received 19th November 2025,
Accepted 27th March 2026

DOI: 10.1039/d5cc06562c

rsc.li/chemcomm

[a] Graduate School of Advanced Science and Technology, Japan Advanced Institute of Science and Technology, 1-1 Asahidai, Nomi, Ishikawa 923-1292, Japan. E-mail: okeyoshi@jaist.ac.jp
[b] Department of Materials Engineering, Graduate School of Engineering, The University of Tokyo, 7-3-1 Hongo, Bunkyo-ku, Tokyo 113-8656, Japan

1. Introduction

Living organisms are open systems that exchange substances and energy with their surroundings. They are nonequilibrium and dissipative systems that maintain a high level of complexity

Kosuke Okeyoshi

Kosuke Okeyoshi is an Associate Professor at JAIST (Japan). He received his PhD in 2010 from The University of Tokyo (Japan). With the support of the Japan Society for the Promotion of Science fellowships DC1, PD, and Research Abroad, he worked at The University of Tokyo, RIKEN (Japan), and Harvard University (United States). He began working at JAIST in 2014, focusing on bioinspired soft materials. He has received several awards, including the Commendation for Science and Technology from the Minister of Education, Culture, Sports, Science, and Technology and the Young Scientists' Award in 2021.

Ryo Yoshida

Ryo Yoshida is a professor at The University of Tokyo, Japan. He received his PhD in 1993 from Waseda University, Japan. He was a research associate at Tokyo Women's Medical University in 1993, a researcher at the National Institute of Materials and Chemical Research from 1994 to 1997, and an assistant professor at the University of Tsukuba from 1997 to 2000. In 2001, he moved to The University of Tokyo as an associate professor, and became a full professor in 2012. He received an award from the Society of Polymer Science, Japan (SPSJ) in 2019, etc.

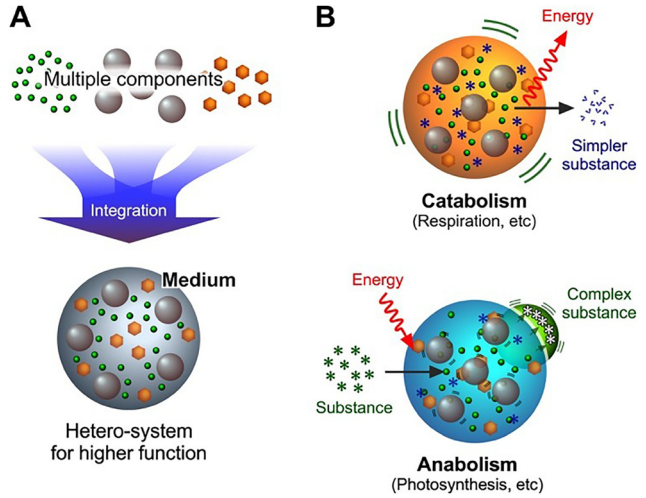

Fig. 1 (A) Schematic describing the integration of multiple components using a soft mediator to enhance functionality. (B) Schematic describing anabolism and catabolism in living systems.

by increasing the entropy in their environments. The emergence of functions in such organisms occurs through heterosystems, which are composed of multiple materials (Fig. 1A). The components are not simply mixed in a homogeneous state but are heterogeneously integrated to achieve functional expression. Such systems contain mediators, which have no direct roles for chemical reactions but have spatial functions in the process. For example, lipid bilayer membranes promote the coexistence and coordination of multiple functional proteins, such as photosystems. ATP-producing mitochondria and photosynthetic chloroplasts are two of the most impressive examples of integrated chemical systems in the cells of higher green plants. These integrated systems are open material systems, enabling the transmission or transformation of energy and substances, *i.e.*, metabolism. Ultimately, the mediator does not chemically react but provides physical environments beyond the molecular hierarchy. To better understand the role of mediators, it is necessary to evaluate their functionality at higher coordination and identify whether their presence is coincidental and/or necessary.[1]

Metabolism is a set of chemical reactions that occur in living organisms, which enable organisms to grow and regenerate their bodies. All forms of metabolism rely on redox reactions involving electron transfer from reduced donors, such as organic molecules or water, to acceptors, such as oxygen. Metabolism is typically categorized into catabolism and anabolism (Fig. 1B). Catabolism breaks down complex organic molecules, *e.g.*, to harvest energy during cellular respiration. In animals, these reactions involve complex organic molecules that are broken down into simpler molecules, such as carbon dioxide and water. Anabolism uses energy to synthesize complex molecules and construct cellular components such as glucose through photosynthesis. In photosynthetic organisms such as plants, electron transfer reactions do not release energy but are used to store energy absorbed from sunlight. Generally, simple precursors are stored and complex molecules with cellular structures are progressively constructed from these precursors.

Soft mediators, such as membranes and polymer networks, are useful for developing metabolism-inspired materials. Soft mediators are the main materials produced during the evolutionary history of living organisms, and are commonly found in cell membranes and the extracellular matrix. Both bilayer membranes and polymer networks can retain multiple components, such as enzymes. Many research groups investigate polymer gels because studies of these materials synergistically strengthen our understanding of physics, chemistry, and life sciences. Breakthroughs in polymer gels occurred in the late 20th century, *i.e.*, the discovery of the volume phase transition of gels[2] and their development into artificial muscles.[3] In the last few decades, bioinspired hydrogels exhibiting similar characteristics or functions as living organisms have been extensively developed.

Previously, we reviewed the topics of self-oscillating gels[4] and artificial photosynthetic gels.[5] To complement this literature, this review overviews two types of gels based on metabolic activities, *i.e.*, catabolism and anabolism. As like the rhythmical heat beating driven by TCA cycle in catabolism, the self-oscillating gels show periodic volume swelling and deswelling driven by Belousov–Zhabotinsky (BZ) reaction. In contrast, as like the photosynthesis of chloroplast driven by Calvin–Benson cycle in anabolism, the artificial photosynthetic gels show photoenergy conversion from water into hydrogen or oxygen through multiple redox reactions driven by an electronic transfer circuit. Although the artificial ones are partially constructed, the approaches provide guidelines for integration of multiple molecules and functional emergence. In this review, the metabolism inspired gels involving chemical reaction circuit are introduced with molecular and systematic strategies. Based on fundamental chemical technologies, various spatial positioning techniques can be used for the multiple components in polymer networks. We discuss integration methodologies for constructing heterosystems exhibiting the emergence of higher function. To highlight these points, the following topics are described: molecular arrangements of functional molecules in networks; the control of the gel shape and size at the microscale; physicochemical advantages of microgels at the nanometer scale; the utilization of the reconstructive ability of proteins; and the precise design of polymer chains at the nanometer scale.

2. Polymer networks with emergence of function

2.1 Bioinspired gels and polymer network designs

Since the discovery of the volume phase transition of polymer gels,[2] many types of energy-converting gels have been developed based on a "from gels to life" strategy.[6] Since gels act as an open material system capable of transforming energy or information, stimulus-responsive gels[7–9] (reacting to temperature, pH, light, solvent composition, ionic strength, electric field, *etc.*) and mechanically tough gels,[10–13] have been developed. Furthermore, information-transforming gels such as chemo-mechanical gels,[14,15] electromechanical gels,[16] and molecular-recognition

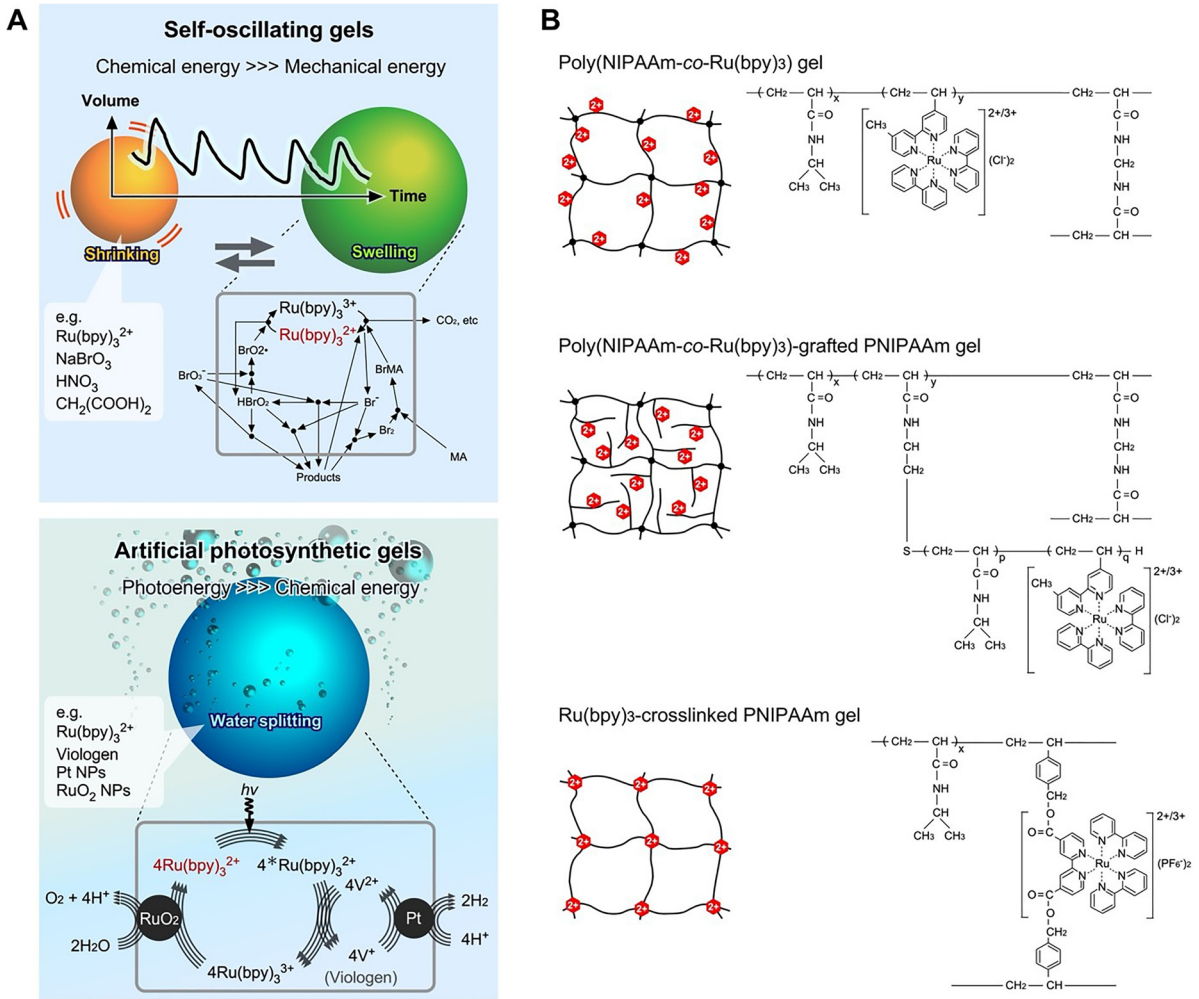

Fig. 2 (A) Concepts of bioinspired self-oscillating gels and artificial photosynthetic gels. (B) Design of polymer networks and chemical structures: poly(NIPAAm-*co*-Ru(bpy)$_3$) gel, poly(NIPAAm-*co*-Ru(bpy)$_3$)-grafted PNIPAAm gel, and Ru(bpy)$_3$-crosslinked PNIPAAm gel.

gels[17] have been demonstrated. These gels convert chemicals from the environment into mechanical energy, *i.e.*, a volume change of the gel. Furthermore, various bioinspired gels have been developed with life-like functions, such as self-healing,[18,19] self-sorting,[20] and mechanical growing,[21] using heterogeneous chemical components in the networks. Thus, the polymer networks have huge potentials to become a mediator for the reaction field, like artificial supramolecules providing the research area of enzyme mimics.[22–24] The sustainable applications in biomedicals and industrials can be expected.

In this review, polymer networks that copolymerize with redox catalysts, such as the Ru(bpy)$_3$ complex and viologen, are summarized as examples of metabolism-inspired gels. As shown in Fig. 2A, the characteristic functions of the gel convert chemical energy to mechanical energy or photoenergy to chemical energy through multiple redox reactions. As examples of catabolism-inspired gels, self-oscillating gels are discussed. These gels convert chemical substances into mechanical oscillations of the volume, similar to a heart beating.[4,15] By copolymerizing a redox catalyst into the network, the hydrogels convert the chemical oscillation of the BZ reaction involving Ru(bpy)$_3$, HNO_3, $NaBrO_3$, and malonic acid, as like TCA cycle that generates the breathing rhythm. The reaction is converted into autonomic swelling/deswelling volume oscillations of the gels under non-oscillatory environment. The gels involve the transducing circuit and continuously show the periodic oscillation until the reactants are consumed. Furthermore, as anabolism-inspired gels, artificial photosynthetic gels are discussed. These gels were developed for splitting water into hydrogen and oxygen *via* photoinduced reactions involving RuO_2/Ru(bpy)$_3$/viologen/Pt.[5] The photoinduced electron transfer circuit are designed in the polymer network to convert visible light energy into high-energy substances like chloroplasts having photosystems on bilayer membranes. Both types of gels work driven by chemical reaction circuits as like TCA circuit or Calvin–Benson cycle. This strategy is called "metabolism-inspired" in this study. Considering that the fundamental functions have been described in previous reviews,[4,5] the methods for preparing the polymer networks are described here.

The Ru(bpy)$_3$ complex plays an important role in the design of both gels. It functions as a redox catalyst in the BZ reaction

and as a photosensitizer in photoinduced chemical reactions. Fig. 2B shows the molecular arrangement of three types of copolymer networks based on the thermoresponsive poly(*N*-isopropylacryamide) (PNIPAAm). PNIPAAm is a stimuli-responsive polymer that exhibits a phase transition at approximately 32 °C in water with a lower critical solution temperature (LCST). Acrylamides have relatively stable chemical properties, mainly seen in the backbone formation of proteins and peptides. Upon copolymerizing the $Ru(bpy)_3$ complex with PNIPAAm, the volume-phase transition temperature differs between the reduced and oxidized states. This is useful for controlling the environment in which the gel exhibits shrunken and swollen states at constant temperature, depending on the redox state. Random copolymer networks can be prepared by radical polymerization using monomers, crosslinkers, and an initiator in a solvent.[15] Self-oscillation gels and artificial photosynthetic gels are developed based on three gel types: poly(NIPAAm-*co*-$Ru(bpy)_3$) (PNR) gel, PNR-grafted PNIPAAm gel, and $Ru(bpy)_3$-crosslinked PNIPAAm gel. Schematics of the polymer network with the $Ru(bpy)_3$ complex are shown to clarify the various molecular arrangements. The characteristics and extensibility of each network are described in the following sections.

Table 1 lists various gels with extended functions, such as acidic conditioning and catalysis for chemical reactions. For the self-oscillating gels, 2-acrylamido-2-methylpropane sulfonic acid (AMPS) is copolymerized to control the acidic conditions for the BZ reaction.[25,26] [3-Methacryloylamino)propyl]trimethylammonium chloride (MAPTAC)[27] or (3-acrylamidopropyl)trimethylammonium chloride (AAPTAC)[28] are copolymerized to add oxidizer-supplying sites by exchanging Cl^- for BrO_3^-. In the case of the artificial photosynthetic gels, Pt nanoparticles (Pt NPs), viologen, and RuO_2 NPs are immobilized or copolymerized to introduce the H_2-generation catalyst, electron acceptor, and O_2-generation catalyst, respectively.[29,30] During the integration of the NPs, the copolymerized $Ru(bpy)_3$ maintains colloidal stability by inhibiting NP aggregation. The electrostatic interactions between cationic $Ru(bpy)_3$ and the NPs protected by the anionic surfactant drive their attraction, but the polymers inhibit the self-aggregation of the NPs. Furthermore, other network designs have been reported that achieve additional functionalization by copolymerization or by controlling the morphologies of the self-assembled structures.[31–35] In the following sections, the basic structures in Fig. 2B are discussed, along with further development steps for integration of function.

2.2 Control of gel shape and size at the micrometer scale

Controlling the shape or size of the gel at the micrometer scale provides a kinetic understanding of the coactive changes in the polymer network that enable energy conversion, such as those in chemo-mechanical gels. To synchronize the volume oscillation rhythm with a constant period, the size of gel needs to be in micrometer scale. At the microscale, gel films on microstructures[36–38] are useful for understanding chemical-wave propagation during the BZ reaction. Film-type bulk gels can be prepared by UV irradiation of a precursor containing a radical initiator. As shown in Fig. 3A, a $Ru(bpy)_3$ crosslinked poly(NIPAAm-*co*-AMPS) gel was prepared onto an epoxy-resin micropost array as a rigid skeleton.[28] When the gel sample was immersed in a BZ reaction solution, an oscillation of color changes propagated continuously. The gels crosslinked by the $Ru(bpy)_3$ complex actively drove the BZ reaction for a long time, and the ligand was stable in a highly acidic aqueous solution. A micropore-type gel was obtained as a freestanding sample by peeling off the gel from the micropost array. The regular array of holes in the gel enables the precise analysis of gel volume changes. The propagated BZ chemical waves resulted in the periodic mechanical contraction and expansion of the gel. This indicates that the $Ru(bpy)_3$ complex crosslinker plays an important role in the redox changes and effective chemomechanical coupling. The volume oscillation and the propagation were clearly observed. A similar oscillation was also confirmed in poly(NIPAAm-*co*-AAPTAC) gels crosslinked with the $Ru(bpy)_3$ complex. In contrast to typical PNR gels crosslinked with methylenebisacrylamide,[15] the swelling behavior of $Ru(bpy)_3$ complex-crosslinked PNIPAAm gels[28] exhibits opposing swelling ratios in the reduced/oxidized states. The swelling ratios are dependent on the molar ratio of the comonomers (AMPS or AAPTAC). These results highlight the modularity of BZ-active metallopolymers.

As shown in Fig. 3B, micrometer-scale spherical gel particles were prepared by suspension polymerization.[39,40] Compared to typical millimeter-scale bulk gels, microscale gel particles have

Table 1 Nano-integration and hetero-functionalization of network structures

	Molecule	Integrated function	Ref.
Poly(NIPAAm-*co*-$Ru(bpy)_3$) gel	—	—	4 and 15
	AMPS	Acid	25 and 26
	MAPTAC	Capture site for oxidant	27
	Pt NPs	H_2 generation catalyst	29
	Viologen	Electron acceptor	29
	RuO_2	O_2 generation catalyst	30
Poly(NIPAAm-*co*-$Ru(bpy)_3$)-grafted PNIPAAm gel	—	—	30
	$Ru(bpy)_3$	Redox catalyst	31
	RuO_2	O_2 generation catalyst	30
$Ru(bpy)_3$-crosslinked PNIPAAm gel	—	—	28
	AMPS	Acid	28
	AAPTAC	Capture site for oxidant	28

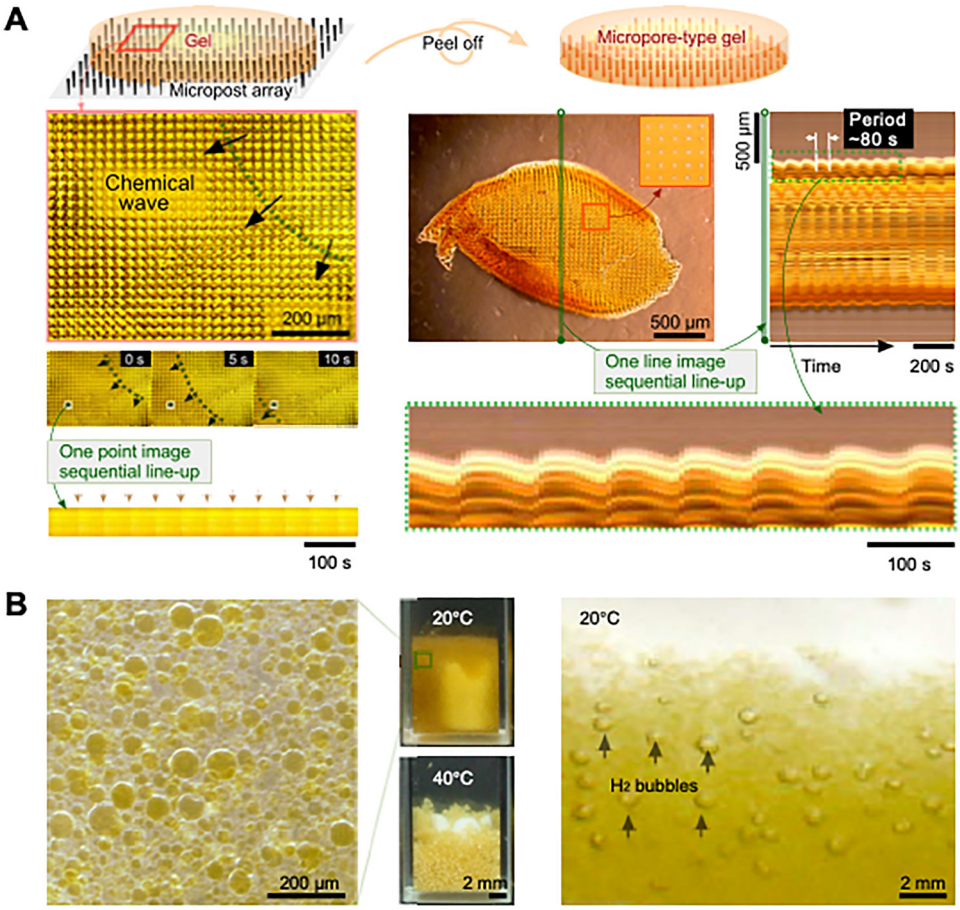

Fig. 3 (A) Demonstrations of self-oscillating systems using $Ru(bpy)_3$-crosslinked poly(NIPAAm-*co*-AMPS) gels. Chemical wave propagation in a gel fixed on a micropost array substrate (diameter: 10 μm, height: 100 μm, pitch: 25 μm) and its volume changes in the free-standing state in a BZ reaction solution. (B) Photoinduced H_2-generation systems based on poly(NIPAAm-*co*-$Ru(bpy)_3$) gels. The images show an aqueous suspension of gel particles. The gel shows volume changes, *i.e.*, swelling at 20 °C and deswelling at 40 °C. Gels containing Pt NPs exhibit H_2 generation in an EDTA solution under visible light. Reproduced from ref. 28 and 39 with permission from Wiley-VCH (Copyright 2018), and the Royal Society of Chemistry (Copyright 2009).

larger surface areas. The smaller gel particles accelerate the initial conditioning of the necessary substances from the external solution. Not only this, generated substances can be easy to go outside. To realize this, gel particles were prepared from an aqueous precursor including NIPAAm, a $Ru(bpy)_3$ monomer, methylenebisacrylamide as a crosslinker, and a Pt-colloidal solution. After adding an initiator to the cooled precursor, it was placed in liquid paraffin as an oil phase and cooled to induce reverse suspension polymerization. After gelation, the samples were thoroughly washed to remove the unreacted compounds. The diameters of the PNR gel particles containing Pt NPs were ~30–100 μm in the swollen state in water.

Photoinduced H_2 generation by an electron-transfer system (EDTA/$Ru(bpy)_3^{2+}$/viologen/Pt) was demonstrated by clarifying the effect of temperature on the polymer network and H_2 generation rate. Owing to the thermo-sensitive PNIPAAm chains, the swollen gel at 20 °C generates H_2 more efficiently than the conventional solution system. In contrast, at 40 °C, the shrunken gel with approximately 0% transmittance generated no H_2. The optimal temperature for efficient H_2 generation was just below the volume-phase-transition temperature (~29 °C). The characteristics of this temperature dependence are similar to the optimum temperature of protein activity. In contrast to the proteins showing irreversible changes in structure at excessively high temperatures, the gel showed reversible H_2 generation behavior, despite being thermally cycled across the volume-phase transition temperature. Furthermore, the ON–OFF switching of photoinduced H_2 generation was controlled by temperature. However, the micrometer scale gels generally have a limitation for the response speed during the swelling/deswelling process. To solve this limitation, there are some strategies including reducing the gel size into submicron/nano meter scale.

2.3 Integration of microgels and nanoparticles

Bioinspired soft materials include functionalized microgels and self-assembled structures,[41,42] such as drug carriers,[43] nanoreactors,[44,45] and photonic crystals.[46,47] Submicron microgels exhibit many advantages, such as high transparency, diffusion rates, surface area, and dispersion stability. In contrast to bulk gels, as described in the previous sections, microgels can form hierarchical structures. PNR microgels were

prepared by precipitation polymerization using a method similar to that for PNIPAAm microgels.[48,49] Microgels with uniform diameters are useful for controlling the synchronous behavior of molecular diffusion inside and outside the polymer network. In addition, colloidal crystals composed of microgels of uniform size, smaller than a target wavelength, are useful for fabricating photonic crystals as optical waveguides. In a first step toward this design, a photoinduced H_2 nano-generator was developed by integrating a photo-sensitizer and catalyst in a polymer network of microgels.

Nano-integration was demonstrated based on the electrostatic interactions among the molecules and the shrinking process of a thermosensitive PNIPAAm network (Fig. 4A).[50,51] First, positively charged PNR microgels and negatively charged Pt NPs protected by anionic surfactants were prepared. By mixing these materials in a swollen gel, the Pt NPs in the surrounding solution can be introduced into the interior of the gel *via* electrostatic interactions. Next, by increasing the temperature while avoiding collapse, the network shrank to physically immobilize the Pt NPs in the interior network. The dispersion was stable (Fig. 4B), and a hetero-nanomaterial was successfully prepared. The TEM images in Fig. 4C show the naturally dried PNR microgels before and after the integration of Pt NPs. The PNR microgels are spherical before integration due to electron absorption by Ru. After integration, PNR microgels with immobilized Pt NPs, with diameters of approximately 2 nm, are clearly observed in the network. The network mesh size should be sufficiently large to capture NPs in a swollen state. By using the dispersion the microgels, efficient H_2 generation was achieved using microgels capable of closely arranging the sensitizer and catalyst. Not only such physical strategies, there also are chemical strategies to provide precise macromolecular arrangements using the chemical strategies such as bio-conjugation or precise synthesis of polymer chain would be reviewed in the following sections.

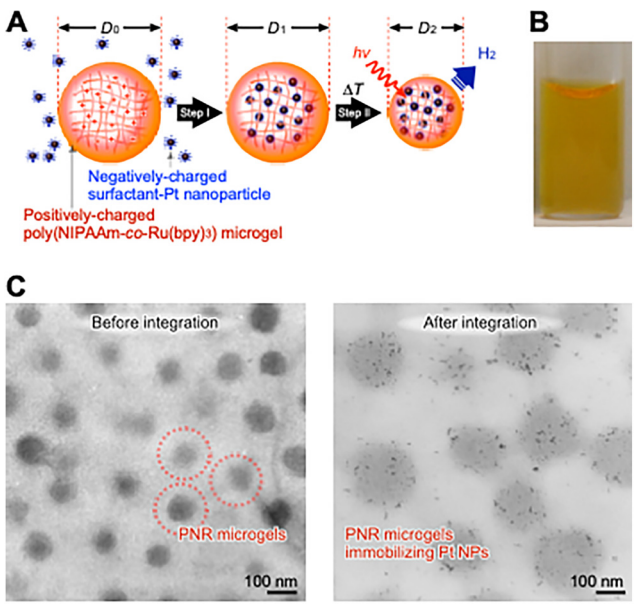

Fig. 4 (A) Nano-integration of poly(NIPAAm-*co*-Ru(bpy)$_3$) microgels and Pt NPs. The positively charged PNR network absorbs the negatively charged Pt NPs (step I), which are immobilized in the thermo-sensitive network by shrinking (step II). (B) Photograph of a dispersion of microgels involving Pt NPs. TEM images of PNR microgels (C) before and after integration with Pt NPs. Reproduced from ref. 50 and 51 with permission from Wiley-VCH (Copyright 2011), and the American Chemical Society (Copyright 2012).

2.4 Conjugation of $Ru(bpy)_3^{2+}$ on microtubules

The metabolic activities in molecular scale are achieved by precisely arranged nanostructures composed of proteins. In particular, supramolecular and polymer nanoarchitectures provide functional advantages, comparing with present synthetic molecules. Microtubules (MTs) play significant roles in many cellular activities, such as mass transportation and neural signal transmission, in the presence of inhibitory factors in the intercellular environment. MTs are one of the cytoskeletal proteins, which exhibit a hierarchical structure resulting from the assembly of α/β-tubulin heterodimer with a diameter of 4 nm. By increasing the temperature to 37 °C, the tubulins form rigid cylindrical filaments composed of 13 heterodimers per loop with an outer diameter of 25 nm, and tens of micrometers in length. MTs reversibly depolymerize to form tubulin when the temperature decreases. The dynamic equilibrium between MT self-assembly and disassembly has been extensively studied. The outer surfaces of MTs are useful for both chemical and physical binding, as exemplified by the motion of kinesin or dynein on the MTs. In addition to their dynamic properties, MTs have huge potential as a mediator for the transmission of specific ions or materials, *e.g.*, as in neural signal transmission. By conjugating functional molecules on tubulin and integrating them into MTs *via* polymerization, optimal molecular arrangements on MTs with suitable distances for electron transferring could be achieved.

Recently, $Ru(bpy)_3^{2+}$-conjugated tubulin was prepared by the amine coupling of $Ru(bpy)_3^{2+}$–succinimidyl ester with primary amine groups on MT surfaces (Fig. 5A), similar to the conjugation of other molecules.[52–57] $Ru(bpy)_3^{2+}$–tubulin was prepared an average $Ru(bpy)_3^{2+}$ molecules/tubulin stoichiometry of 3.1/2.0.[58–60] The efficiency of labeling by amine coupling was 31%. As shown in Fig. 5B, $Ru(bpy)_3^{2+}$–MTs were purified by ultracentrifugation and recovered from the bottom of the centrifuge tube. Fluorescence microscopy revealed MT fibers with a length of 20–50 μm in the 5 μm gap between two glass cover slips (Fig. 5C). The fluorescence originates from the nonradiative process of excited $Ru(bpy)_3^{2+}$, $^*Ru(bpy)_3^{2+}$. The transition curves as a function of temperature for tubulins/MTs are summarized in Fig. 5D, based on the kinetics of the polymerization of tubulins to MTs. In comparison with non-conjugated tubulin, $Ru(bpy)_3^{2+}$-conjugated tubulin showed a lower temperature at which tubulin polymerized into MTs. Interestingly, the photoirradiation of $Ru(bpy)_3^{2+}$–tubulin enhanced MT formation at 25 and 30 °C, whereas polymerization enhancement was not observed at all for non-conjugated tubulin. It can be speculated that the excited $Ru(bpy)_3^{2+}$ releases thermal energy non-radiatively *i.e.*, $^*Ru(bpy)_3^{2+} \rightarrow Ru(bpy)_3^{2+}$ + heat,[61–63]

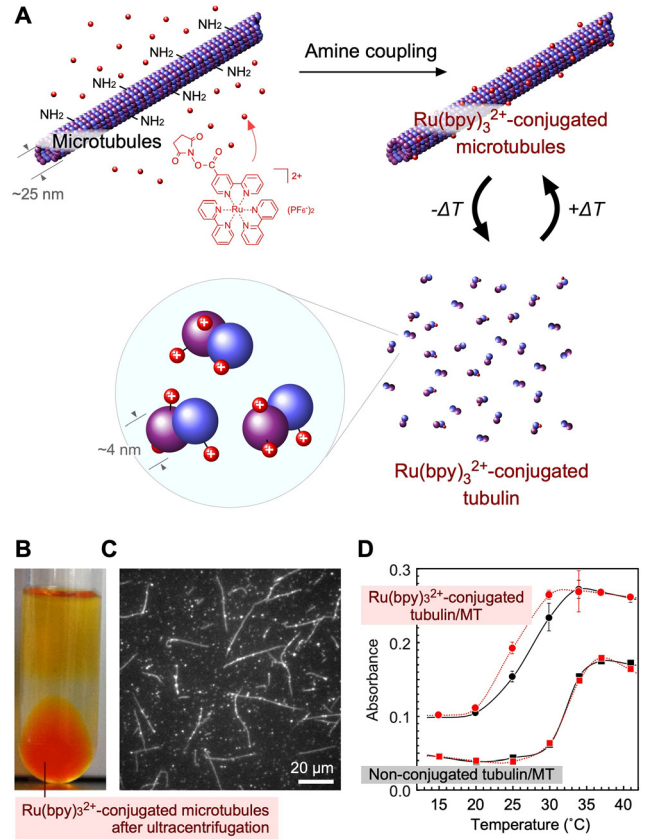

Fig. 5 (A) Schematic of $Ru(bpy)_3^{2+}$-conjugated tubulin and MTs. (B) Purification of $Ru(bpy)_3^{2+}$–MTs through ultracentrifugation. (C) Fluorescence microscopy image of $Ru(bpy)_3^{2+}$–MTs. (D) Transition curves of tubulin/MTs as a function of temperature. Each plot shows the absorption strength at 350 nm, 20 min after the temperature was changed from 3 °C to various temperatures. Black plot and line correspond to the non-irradiated samples and the red plot and line correspond to the irradiated samples. Reproduced from ref. 58 with permission from the Royal Society of Chemistry, Copyright 2014.

increasing the local temperature around $Ru(bpy)_3^{2+}$–tubulin. Thus, $Ru(bpy)_3^{2+}$–tubulin acts as a photothermal energy sensitizer that promotes assembly.

As another nonradiative process, electron transferring to other molecules is useful for photoinduced chemical reactions. For example, $Ru(bpy)_3^{2+}$–MTs act as a photoinduced electron-generating network. First, the effect of $Ru(bpy)_3^{2+}$–tubulin/MT polymerization on photoinduced H_2 generation were focused. Although $Ru(bpy)_3^{2+}$–tubulin flocculated into a disordered state in the reaction mixture (EDTA/$Ru(bpy)_3^{2+}$/MV^{2+}/Pt), $Ru(bpy)_3^{2+}$–MTs maintained the network structure.[59,60] Furthermore, the MTs maintained their structure during photochemical reactions. Owing to their structural stability, $Ru(bpy)_3^{2+}$–MTs exhibited more effective H_2 generation than a $Ru(bpy)_3^{2+}$–tubulin flocculation. Thus, the hierarchical structure allows effective electron transfer for forward reactions. This MT-based reaction field has potential use in close molecular arrangements by integrating functional molecule-conjugated tubulins to enable applications such as artificial photosynthetic organisms and photoinduced actuators.

2.5 Copolymerization of viologen

In actual photosystems of chloroplast, quinone derivatives act as an electron transporter by the redox processes. One of artificial molecules for the similar function, viologens capable of redox changes can be covalently linked with other functional molecules or incorporated into polymer chains to fabricate functional materials. Typical systems in photochemistry and electrochemistry include electron relay systems and molecular shuttles.[64–70] In this review, random copolymerization was used as the basic method for preparing polymers containing viologen units as the electron acceptor. The chemical structures of three copolymers and poly(NIPAAm-*co*-$Ru(bpy)_3$-*co*-viologen) gel (PNRV gel)[26] are shown in Fig. 6A. To prepare artificial photosynthetic gels, the viologen unit can also be introduced into the network as a PNRV gel containing Pt NPs. Under visible irradiation, the color of the gel changes from orange to blue as the reduced state of viologen increases (Fig. 6B), suggesting that electrons are transferred from $Ru(bpy)_3^{2+}$ to viologen in the polymer network. Simultaneously, H_2 gas was continuously generated, suggesting that electrons were transferred effectively among the three components in the gel. However, the H_2 generation rate in this system was thousands of times lower than that of PNR gel systems using free methylviologen. This is mainly because $Ru(bpy)_3^{2+}$ and viologen are copolymerized randomly in PNIPAAm-based chains, and most viologens are too far from the Pt NPs to transfer electrons to them. Therefore, Ru and viologens should be independently immobilized in the polymer network using other molecular strategies.

Considering this problem, viologen units were designed as linear polymers, such as poly(NIPAAm-*co*-viologen) (PNV)[71] and poly(NIPAAm-*co*-AAm-*co*-viologen) (PNAV)[72] (Fig. 6A). Semi-telechelic PNV and PNAV with a terminal amino group were synthesized by the radical telomerization of NIPAAm, AAm, and the viologen monomer using 2-aminoethanethiol (AESH) as a chain-transfer agent. The molecular structure of the viologen monomer was designed to introduce an acrylamide group to induce characteristics similar to those of NIPAAm. The degree of polymerization was controlled by varying the amount of AESH. The molecular weights of the polymers, determined by gel permeation chromatography, were in the range of 5–10 × 10^3 g mol^{-1}. The amount of viologen units introduced into the copolymers was approximately 5 mol% for a composition of 10 mol%. As shown in Fig. 6B, the aqueous solutions of PNV and PNAV were colorless in the oxidized state (PNV^{2+} and $PNAV^{2+}$) and violet in the reduced state (PNV^{+} and $PNAV^{+}$). The maximum absorption in the reduced state occurred at wavelengths of approximately 530 and 550 nm, similar to that of the viologen monomer. This absorption does not interfere with the absorption of the $Ru(bpy)_3^{2+}$ photosensitizer, with maximum absorption at a wavelength of ~450 nm.

2.6 Active electron transportation by coil-globule transition

Fig. 7A shows the temperature dependence of the transmittance changes for the PNV and PNAV solutions.[71,72] The redox states of viologen in the polymers were controlled using

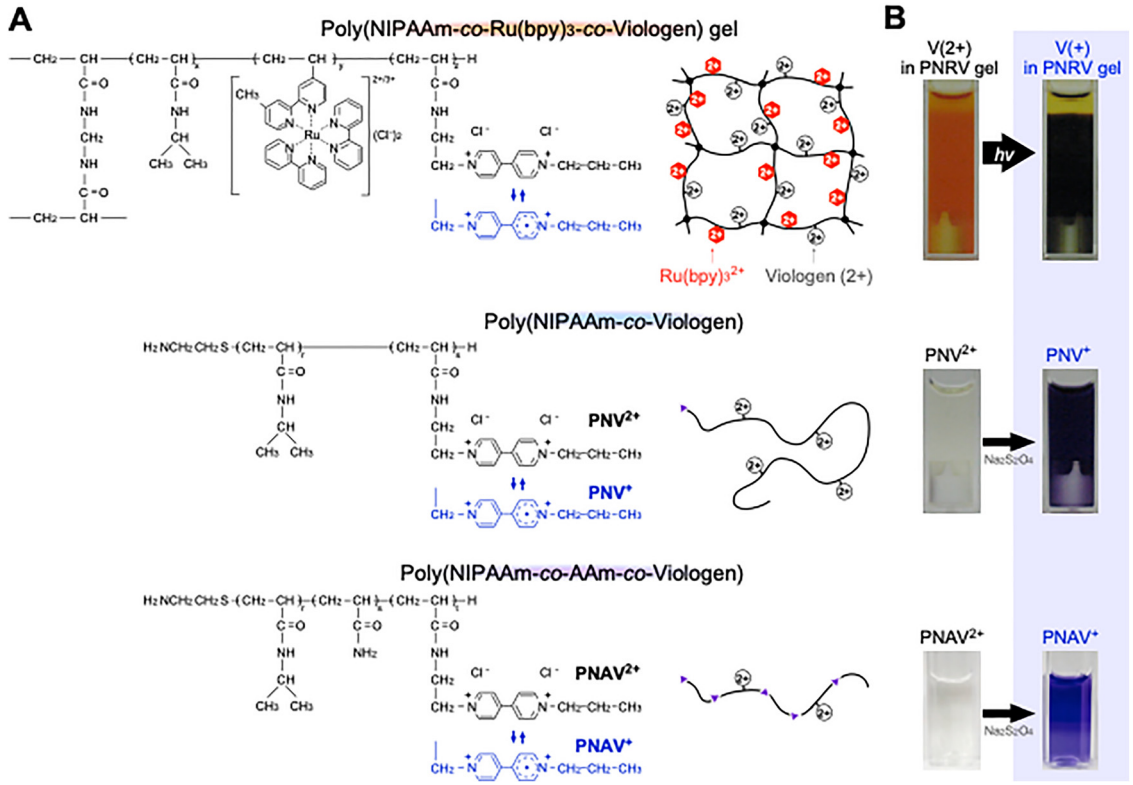

Fig. 6 (A) Chemical structures and schematic polymer structures of poly(NIPAAm-*co*-Ru(bpy)$_3$-*co*-viologen) gel, poly(NIPAAm-*co*-viologen) (PNV), and poly-(NIPAAm-*co*-AAm-*co*-viologen) (PNAV). (B) Photographs of gel particle suspensions or polymer solutions with viologen in the (left) oxidized state (V^{2+}) and (right) reduced state (V^{+}). Reproduced from ref. 26, 71 and 72 with permission from the Royal Society of Chemistry (Copyright 2009, 2024) and Wiley-VCH (Copyright 2019).

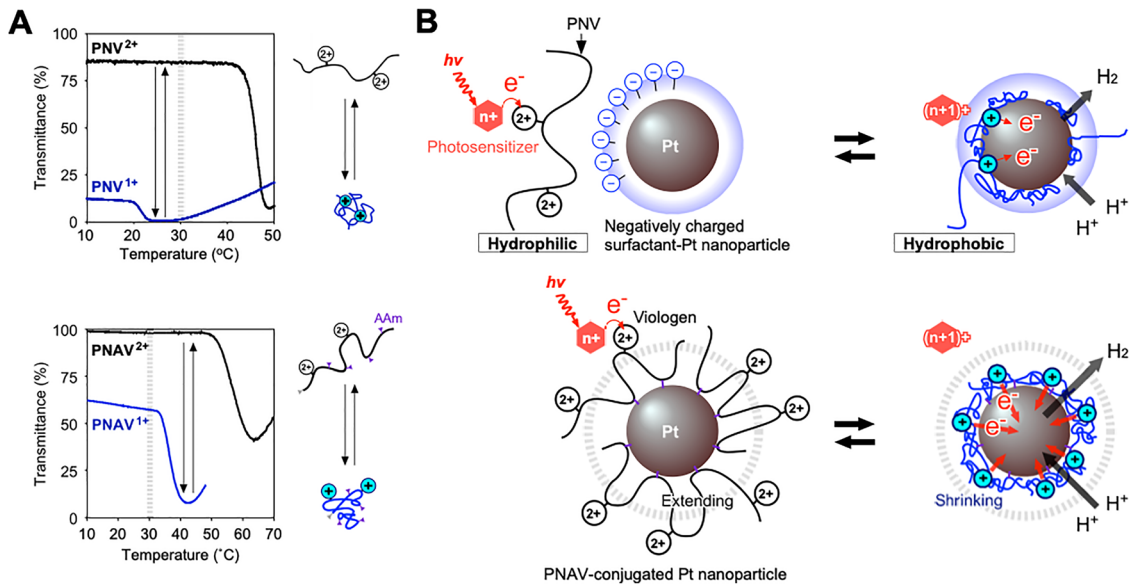

Fig. 7 (A) Temperature dependence of the transmittance of (top) $PNV^{2+/+}$ and (bottom) $PNAV^{2+/+}$ solutions. Schematics showing the extending/shrinking states of the polymer. (B) Schematics of the photoinduced H_2 generation system involving electron transfer driven by coil-globule transitions on Pt NPs in the PNV and PNAV systems. Reproduced from ref. 71 and 72 with permission from Wiley-VCH (Copyright 2019) and the Royal Society of Chemistry (Copyright 2024).

$Na_2S_2O_4$ as a reductant. As the temperature increased, the transmittance suddenly decreased because of the thermosensitivity of PNIPAAm, indicating a phase transition at the LCST. When the viologen units were kept in the reduced state (PNV^+ and $PNAV^+$), the LCSTs were lower than that in the oxidized state (PNV^{2+} and $PNAV^{2+}$). It was due to the enhanced hydrophobicity resulting from the decrease in the charge of the viologen unit. The ionic group enhances the hydrophilicity of

the polymer, whereas the propyl group in the viologen unit enhances its hydrophobicity. For PNAV, the LCST was much higher than that of homo-PNIPAAm, 30 °C in both states. This is likely due to the effect of the AAm unit, which makes the polymer more hydrophilic. Considering the distinct LCSTs of PNV^{2+}/PNV^{+} and $PNAV^{2+}/PNAV^{+}$, it is expected that the polymer will exhibit cyclic changes in expansion/shrinkage when the viologen unit is oxidized and reduced cyclically in a photo-induced electron transfer circuit at constant temperature.

In the case of PNV, the polymeric coil-globule transitions with hydrophilic/hydrophobic changes accelerated cyclic electron transfer for H_2 generation (Fig. 7B). In contrast to conventional solution systems (reducer/photosensitizer/electron-acceptor/catalyst), the PNV system exhibits an active electron-transport mechanism based on: (I) conformational changes in PNV driven by redox changes in viologen and (II) close molecular arrangement by electrostatic interactions between the positively charged PNV and the negatively charged Pt NPs dispersed using an anionic surfactant. In this system, when the photoexcited sensitizer $*Ru(bpy)_3^{2+}$ donates an electron to the viologen in the PNV, the reduced viologen causes the polymer to shrink and approach the hydrophobic space on the surface of the Pt NPs. H_2 was generated with an efficiency of ~13% from the accumulated electrons in the Pt NPs and nearby protons. After providing electrons to the Pt NPs, the polymer expanded again, and the circuit operated continuously. However, the PNV system has some limitations. When the viologen in the free PNV far from the Pt NP is in a reduced state, it shrinks and readily flocculates with the neighboring PNV, making it difficult to transfer electrons in the forward reaction.

To resolve this problem, a polymeric system with a precise molecular arrangement is required to remove free PNV. One strategy involves the conjugation of a polymer onto the surface of the Pt NPs to facilitate active electron transfer and the development of a novel catalytic system. As shown in Fig. 7A and B, a copolymer-conjugated nanocatalytic system for active electron transfer using a ternary random copolymer, PNAV, was developed. Using copolymerized acrylamide (AAm), PNAV was conjugated to Pt NP surfaces. The PNAV-conjugated Pt NPs were designed for active electron transport in the H_2-generation reaction. When the copolymerized viologen undergoes redox changes, the polymeric coil-globule transitions result in cyclic swelling and shrinking, thereby using photoenergy and generating H_2. Unlike the PNV system, the PNAV system was precisely arranged on the nanometer scale for electron transfer. According to Marcus theory, electrons transfer more effectively when the distance between an electron donor and acceptor is below ~2 nm.[73,74] In the PNAV system, when a photoexcited sensitizer such as $*Ru(bpy)_3^{2+}$ donates an electron to viologen, the reduced viologen triggers the immediate shrinkage of the polymer, causing it to approach the surface of the Pt NPs and enable H_2 generation. Subsequently, the polymer expands again, enabling the electron transfer process to continue. Throughout viologen redox cycles, the polymer chain acts as a distance regulator and an electron-transport medium. This kind of active transportation can be realized by multiple functional molecules with control of the optimum distance between them. Otherwise, the self-quenching or self-aggregation accelerate to inhibit the forward reactions. In the actual photosystems composed of multiple functionals groups work on bilayer membranes with ~8 nm thickness. The excited electrons are given to quinones and the cyclic redox reactions are achieved with the simultaneous transportation of 48 electrons to produce one glucose as the fixation of carbon dioxide.

3. Conclusions and outlook

Inspired by metabolic processes in living organisms, methodologies for integrating multiple molecules to construct heterosystems were discussed, focusing on self-oscillating and artificial photosynthetic gels. Polymer networks are advantageous for the molecular arrangement of multiple components. The network itself acts as a mediator for the reaction field and also actively expands/shrinks *via* a phase transition. The copolymerization of functional molecules in PNIPAAm is strategically important for chemomechanical transduction or coil-globule transitions for active electron transport. In particular, it is possible to immobilize the $Ru(bpy)_3$ complex onto the polymer network as a monomer, macromonomer, or cross-linker. In addition, PNIPAAm-based copolymers with viologens can be prepared by controlling their molecular weights through telomerization. The polymer networks described in this study were prepared *via* simple random copolymerization. Using recent technologies for precise synthesis, such as block copolymerization[75] and alternating copolymerization,[76,77] advanced molecular systems were demonstrated, similar to proteins with precise ternary and quaternary molecular structures. Furthermore, it is expected that the discussed microgels and MTs with nano/submicron scales will facilitate various strategies for integrating functional molecules. As for the present polymer system for the water splitting have been partially constructed, however, the active electron transferring would be one of the significant strategies to completely construct the system. Although the systems are in the developing stage, the active control of the multiple kinds of functional molecules would be essential. As for not only the artificial photosynthetic gels but also self-oscillating gels, by using the recent systematic strategies, design of the hierarchical structures would overcome the limitation. The network structures in large scale as bulk gels have problems such as low diffusions, discharge of oxygen, or no synchronization. Considering that the network structures in nanoscale are enough to drive the chemical reactions, the forms of vesicles and colloidosomes in mesoscale would be useful to solve the problems. Beyond the integration of multiple components, we expect that future heterosystems will exhibit emergent evolution, as seen in natural products.

Conflicts of interest

There are no conflicts to declare.

Data availability

No primary research results, software or code have been included and no new data were generated or analysed as part of this review.

Acknowledgements

This study was supported by a Grant-in-Aid for Challenging Research (Exploratory) (grant number: JP21K18998) from The Ministry of Education, Culture, Sports, Science and Technology (MEXT), Japan.

References

1 J. Monod, *Chance and Necessity: An Essay on the Natural Philosophy of Modern Biology*, Alfred A. Knopf, New York, 1971.
2 T. Tanaka, *Phys. Rev. Lett.*, 1978, **40**, 820–823.
3 Y. Osada and J. P. Gong, *Adv. Mater.*, 1998, **10**, 827–837.
4 R. Yoshida, *Adv. Mater.*, 2010, **22**, 3463–3483.
5 R. Hagiwara, R. Yoshida and K. Okeyoshi, *Chem. Commun.*, 2024, **60**, 13314–13324.
6 T. Tanaka, *From Gels to Life*, University of Tokyo Press, Tokyo, Japan, 2004.
7 S. Katayama, Y. Hirokawa and T. Tanaka, *Macromolecules*, 1984, **17**, 2641–2643.
8 S. Hirotsu, Y. Hirokawa and T. Tanaka, *J. Chem. Phys.*, 1987, **87**, 1392–1395.
9 R. Yoshida, K. Uchida, Y. Kaneko, K. Sakai, A. Kikuchi, Y. Sakurai and T. Okano, *Nature*, 1995, **374**, 240–242.
10 Y. Okumura and K. Ito, *Adv. Mater.*, 2001, **13**, 485–487.
11 K. Haraguchi and T. Takehisa, *Adv. Mater.*, 2002, **14**, 1120–1124.
12 J. P. Gong, Y. Katsuyama, T. Kurokawa and Y. Osada, *Adv. Mater.*, 2003, **15**, 1155–1158.
13 T. Sakai, T. Matsunaga, Y. Yamamoto, C. Ito, R. Yoshida, S. Suzuki, N. Sasaki, M. Shibayama and U. Chung, *Macromolecules*, 2008, **41**, 5379–5384.
14 E. Kokufuta and T. Tanaka, *Macromolecules*, 1991, **24**, 1605–1607.
15 R. Yoshida, T. Takahashi, T. Yamaguchi and H. Ichijo, *J. Am. Chem. Soc.*, 1996, **118**, 5134–5135.
16 Y. Osada, H. Okuzaki and H. Hori, *Nature*, 1992, **355**, 242–244.
17 T. Miyata, N. Asami and T. Uragami, *Nature*, 1999, **399**, 766–769.
18 Q. Wang, J. L. Mynar, M. Yoshida, E. Lee, M. Lee, K. Okuro, K. Kinbara and T. Aida, *Nature*, 2010, **463**, 339–343.
19 M. Nakahata, Y. Takashima, H. Yamaguchi and A. Harada, *Nat. Commun.*, 2011, **2**, 511.
20 S. Onogi, H. Shigemitsu, T. Yoshii, T. Tanida, M. Ikeda, R. Kubota and I. Hamachi, *Nat. Chem.*, 2016, **8**, 743–752.
21 T. Matsuda, R. Kawakami, R. Namba, T. Nakajima and J. P. Gong, *Science*, 2019, **363**, 504–508.
22 M. J. Wiester, P. A. Ulmann and C. A. Markin, *Angew. Chem., Int. Ed.*, 2010, **50**, 114–137.
23 H. Wei and E. Wang, *Chem. Soc. Rev.*, 2013, **42**, 6060–6093.
24 H. Yu, M. Eres, S. L. Hilburg, P. Kang, T. Jin, A. Grigoropoulos, Z. Li, D. M. Loh, I. Jayapurna, Z. Ruan, W. Fu, F. Yang, P. Ganesh, K. Toste, S. Li, J. Guo, H. Huang, F. D. Toste, R. D. Britt, Y. Z, A. Alexander-Katz and T. Xu, *Nature*, 2026, **649**, 83–90.
25 Y. Hara and R. Yoshida, *J. Phys. Chem. B*, 2005, **109**, 9451–9454.
26 Y. Murase, S. Maeda, S. Hashimoto and R. Yoshida, *Langmuir*, 2009, **25**, 483–489.
27 Y. Hara, T. Sakai, S. Maeda, S. Hashimoto and R. Yoshida, *J. Phys. Chem. B*, 2005, **109**, 23316–23319.
28 M. Aizenberg, K. Okeyoshi and J. Aizenberg, *Adv. Funct. Mater.*, 2018, **28**, 170425.
29 K. Okeyoshi and R. Yoshida, *Soft Matter*, 2009, **5**, 4118–4123.
30 K. Okeyoshi and R. Yoshida, *Adv. Funct. Mater.*, 2010, **20**, 708–714.
31 R. Mitsunaga, K. Okeyoshi and R. Yoshida, *Chem. Commun.*, 2013, **49**, 4935–4937.
32 Y. Zhang, N. Zhou, S. Akella, Y. Kuang, D. Kim, A. Schwartz, M. Bezpalko, B. M. Foxman, S. Fraden, I. R. Epstein and B. Xu, *Angew. Chem., Int. Ed.*, 2018, **52**, 11494–11498.
33 T. Yamamoto and R. Yoshida, *React. Funct. Polym.*, 2013, **73**, 945–950.
34 T. Masuda, T. Ueki, R. Tamate, K. Matsukawa and R. Yoshida, *Angew. Chem., Int. Ed.*, 2018, **57**, 16693–16697.
35 T. Ueno, K. Bundo, Y. Akagi, T. Sakai and R. Yoshida, *Soft Matter*, 2010, **6**, 6072–6074.
36 B. Pokroy, A. K. Epstein, M. C. M. Persson-Gulda and J. Aizenberg, *Adv. Mater.*, 2009, **21**, 463–469.
37 B. Pokroy, S. H. Kang, L. Mahadevan and J. Aizenberg, *Science*, 2009, **323**, 237–240.
38 L. Zarzar, P. Kim and J. Aizenberg, *Adv. Mater.*, 2012, **23**, 1442–1446.
39 K. Okeyoshi and R. Yoshida, *Chem. Commun.*, 2009, 6400–6402.
40 K. Okeyoshi and R. Yoshida, *Chem. Commun.*, 2011, **47**, 1527–1529.
41 R. Pelton, *Adv. Colloid Interface Sci.*, 2000, **85**, 1–33.
42 H. Kawaguchi, *Prog. Polym. Sci.*, 2000, **25**, 1171–1210.
43 S. Nayak and L. A. Lyon, *Angew. Chem., Int. Ed.*, 2005, **44**, 7686–7708.
44 J. Zhang, S. Xu and E. Kumacheva, *J. Am. Chem. Soc.*, 2004, **126**, 7908–7914.
45 Y. Lu, Y. Mei, M. Drechsler and M. Ballauff, *Angew. Chem., Int. Ed.*, 2006, **45**, 813–816.
46 J. M. Weissman, H. B. Sunkara, A. S. Tse and S. A. Asher, *Science*, 1996, **274**, 959–963.
47 Z. Hu, X. Lu and J. Gao, *Adv. Mater.*, 2001, **13**, 1708–1712.
48 D. Suzuki, T. Sakai and R. Yoshida, *Angew. Chem., Int. Ed.*, 2008, **47**, 917–920.
49 D. Suzuki, H. Taniguchi and R. Yoshida, *J. Am. Chem. Soc.*, 2009, **131**, 12058–12059.
50 K. Okeyoshi, D. Suzuki, A. Kishimura and R. Yoshida, *Small*, 2011, **7**, 311–315.
51 K. Okeyoshi, D. Suzuki and R. Yoshida, *Langmuir*, 2012, **28**, 1539–1544.
52 J. B. Olmsted and G. G. Borisy, *Biochemistry*, 1973, **12**, 4282–4289.
53 D. K. Fygenson, E. Braun and A. Libchaber, *Phys. Rev. E: Stat. Phys., Plasmas, Fluids, Relat. Interdiscip. Top.*, 1994, **50**, 1579–1588.
54 J. Howard, *Mechanics of Motor Proteins and the Cytoskeleton*, Sinauer Associates, Sunderland, MA, 2001.
55 B. Alberts, A. Johnson, J. Lewis, M. Raff, K. Roberts and P. Walter, *Molecular Biology of the Cell*, Garland Science, New York, 4th edn, 2002.
56 K. I. Sano, R. Kawamura, T. Tominaga, H. Nakagawa, N. Oda, K. Ijiro and Y. Osada, *Biomacromolecules*, 2011, **12**, 1409–1413.
57 K. Okeyoshi, R. Kawamura, R. Yoshida and Y. Osada, *Sci. Rep.*, 2015, **5**, 9581.
58 K. Okeyoshi, R. Kawamura, R. Yoshida and Y. Osada, *J. Mater. Chem. B*, 2014, **2**, 41–45.
59 K. Okeyoshi, R. Kawamura, R. Yoshida and Y. Osada, *Chem. Commun.*, 2015, **51**, 11607–11610.
60 K. Okeyoshi, R. Kawamura, R. Yoshida and Y. Osada, *Langmuir*, 2016, **32**, 626–631.
61 J. V. Caspar and T. J. Meyer, *J. Am. Chem. Soc.*, 1983, **105**, 5583–5590.
62 J. Van Houten and R. J. Watts, *J. Am. Chem. Soc.*, 1976, **98**, 4853–4858.
63 B. Happ, A. Winter, M. D. Hager and U. S. Schubert, *Chem. Soc. Rev.*, 2012, **41**, 2222–2255.
64 T. Matsuo, T. Sakamoto, K. Takuma, K. Sakura and T. Ohsako, *J. Phys. Chem.*, 1981, **85**, 1277–1279.
65 T. Nishijima, T. Nagamura and T. Matsuo, *J. Polym.*, 1981, **19**, 65–73.
66 M. Sykora, K. A. Maxwell, J. M. DeSimone and T. J. Meyer, *Proc. Natl. Acad. Sci. U. S. A.*, 2000, **97**, 7687–7691.
67 H. Murakami, A. Kawabuchi, R. Matsumoto, T. Ido and N. Nakashima, *J. Am. Chem. Soc.*, 2005, **127**, 15891–15899.
68 V. Sindelar, S. Silvi and A. E. Keifer, *Chem. Commun.*, 2006, 2185–2187.
69 H. Zhou, F. Matoba, R. Matsuno, Y. Wakayama and T. Yamada, *Adv. Mater.*, 2023, **35**, 36.
70 K. Imato, T. Hino, N. Kaneda, I. Imae, N. Shida, S. Inagi and Y. Ooyama, *Small*, 2024, **20**, 235067.
71 K. Okeyoshi and R. Yoshida, *Angew. Chem., Int. Ed.*, 2019, **58**, 7304–7307.
72 R. Hagiwara, S. Nishimura and K. Okeyoshi, *Chem. Commun.*, 2024, **60**, 280–283.
73 R. A. Marcus, *Annu. Rev. Phys. Chem.*, 1964, **15**, 155–196.
74 R. A. Marcus and N. Sutin, *Biochim. Biophys. Acta*, 1985, **811**, 265–322.
75 H. Dau, G. R. Jones, E. Tsogtgerel, D. Nguyen, A. Keyes, Y. S. Liu, H. Rauf, E. Ordonez, V. Puchelle, H. B. Basbug Alhan, C. Zhao and E. Harth, *Chem. Rev.*, 2022, **122**, 14471–14553.
76 J. Huang and S. R. Turner, *Polymer*, 2017, **116**, 572–586.
77 K. Nishimori and M. Ouchi, *Chem. Commun.*, 2020, **56**, 3473–3483.

